Environmental Science and Pollution Research (2020) 27:24531–24541
https://doi.org/10.1007/s11356-020-08794-1

RESEARCH ARTICLE

A comparative study of UV/H_2O_2 and UV/PDS for the degradation of micro-pollutants: kinetics and effect of water matrix

Jing Gao[1] · Congwei Luo[1] · Lu Gan[2] · Daoji Wu[1] · Fengxun Tan[1] · Xiaoxiang Cheng[1] · Weiwei Zhou[1] · Shishun Wang[1] · Fumiao Zhang[1] · Jun Ma[3]

Received: 11 September 2019 / Accepted: 6 April 2020 / Published online: 19 April 2020

Abstract

Organic micro-pollutants such as pesticides and endocrine disruptors cause serious harm to human health and aquatic ecosystem. In this study, the potential degradation of atrazine (ATZ), triclosan (TCS), and 2,4,6-trichloroanisole (TCA) by UV-activated peroxydisulfate (UV/PDS) and UV-activated H_2O_2 (UV/H_2O_2) processes were evaluated under different conditions. Results showed that UV/PDS process was more effective than UV/H_2O_2 under the same conditions. Increasing oxidant dosage or decreasing the initial ATZ, TCS, and TCA concentrations promoted the degradation rates of these three compounds. The presence of natural organic matter (NOM) could effectively scavenge sulfate radical ($SO_4^{\bullet-}$) and hydroxyl radical (HO•) and reduced the removal rates of target compounds. Degradation rates of ATZ and TCA decreased with pH increasing from 5.0 to 9.0 in UV/PDS process, while in UV/H_2O_2 process, the increase of solution pH had little effect on ATZ and TCA degradation. In the UV/PDS and UV/H_2O_2 oxidation process, when the solution pH increased from 5 to 8, the removal rates of TCS decreased by 19% and 1%, while when the solution pH increased to 9, the degradation rates of TCS increased by 23% and 17%. CO_3^{2-}/HCO_3^- had a small inhibitory effect on ATZ and TCA degradation by UV/H_2O_2 and UV/PDS processes but promoted the degradation of TCS significantly (> 2 mM). Cl^- had little effect on the degradation of ATZ, TCA, and TCS in UV/H_2O_2 process. Cl^- significant inhibited on the degradation of ATZ and TCS, but the influence of Cl^- on the degradation of TCA was weak in UV/PDS process. Based on these experimental results, the various contributions of those secondary radicals (i.e., carbonate radical, chlorine radical) were discussed. This study can contribute to better understand the reactivities when UV/PDS and UV/H_2O_2 are applied for the treatment of micro-pollutant-containing waters.

Keywords Organic micro-pollutants · Persulfate · H_2O_2 · Ultraviolet · Degradation kinetics

Introduction

With the rapid development of modern industry, more and more organic micro-pollutants have been frequently detected in aquatic environment (Shao et al. 2009; Tobergte and Curtis 2013). Most micro-pollutants have strong water solubility, long half-life, and bioaccumulation (Richardson and Ternes 2005; Huerta-Fontela et al. 2011). These organic micro-pollutants are of great concern because of their potential damage to water environment and human health (Richardson and Ternes 2005). It was pointed out that prolonged exposure to a common pesticide produced behavioral and neuropathological features of Parkinson's disease, and musty odor compounds in drinking water greatly affected the esthetic quality of drinking water and consumer acceptability (Betarbet et al. 2000; Sung et al. 2005; Peter and Von Gunten 2007). Furthermore, some endocrine disruptors have been found in human breast milk, which has adverse effects on human reproduction, immunity, nerve development, and function (Main et al. 2005). Thus, the effective degradation of organic micro-pollutants in water treatment processes has become an important issue.

Responsible Editor: Vítor Pais Vilar

✉ Congwei Luo
luocongwei2009@163.com

✉ Daoji Wu
wdj@sdjzu.edu.cn

[1] School of Municipal and Environmental Engineering, Shandong Jianzhu University, Jinan 250010, China

[2] Shandong Electric Power Engineering Consulting Institute Corp., LTD., Jinan 250010, China

[3] State Key Laboratory of Urban Water Resource and Environment, Harbin Institute of Technology, Harbin 150090, China

Conventional water and wastewater treatment processes (e.g., coagulation, filtration, and biological treatment) were shown to be unable to remove these micro-pollutants effectively (Huerta-Fontela et al. 2011). Fortunately, advanced oxidation processes (AOPs) have proven effective in water treatment for the removal of micro-pollutants (Haag and Yao 1992; Ahmed and Chiron 2014; Luo et al. 2015). The conventional AOPs rely on in situ generation of highly reactive and non-selective radicals (i.e., HO•) for the rapid oxidation of a wide range of organic contaminants. The AOPs include processes such as UV/H_2O_2, Fe^{2+}/H_2O_2, and ozone. (Can and Çakır 2010; Yang et al. 2010; He et al. 2012; Rodríguez-Chueca et al. 2016). Many pharmaceuticals react with HO• at a secondary reaction rate of 10^8 to 10^{10} M^{-1} s^{-1}, and the main mechanism is hydrogen abstraction, electrophilic addition, and electron transfer reactions (Haag and Yao 1992; Huber et al. 2003; Deng et al. 2013).

Recently, sulfate radical (SO_4•$^-$)–based AOPs have attracted significant attention for the degradation of various organic pollutants (Lutze et al. 2015). SO_4•$^-$ is usually generated from activation of persulfate by heat, ferrous iron catalysis, and UV light (Yang et al. 2010; Bennedsen et al. 2012; Kattel et al. 2017). Compared with the non-selective HO• (1.8–2.8 V vs.NHE), SO_4•$^-$ has a higher oxidizing power (2.5–3.1 V vs. NHE) and longer half-life (Luo et al. 2015). SO_4•$^-$ degrade target pollutants mainly through electron transfer reactions, hydrogen abstraction, and addition mechanisms. However, the selectivity of SO_4•$^-$ through electron transfer is stronger than HO• (Xu and Li 2010; Liu et al. 2012). According to some recent reports, SO_4•$^-$ react with certain organic compounds at a higher rate than HO• (Xie et al. 2015; Liu et al. 2018). Thus, reactivity and energy efficiency of SO_4•$^-$ -based oxidation processes may also be different from HO•-based oxidation processes.

Furthermore, various background components in water, such as CO_3^{2-}/HCO_3^-, Cl^-, and natural organic matter (NOM), would scavenge HO• and/or SO_4•$^-$ with different rates, which may lead to various effects on the degradation of target organic compounds in HO•-based and SO_4•$^-$-based oxidation processes. Considering different substances have different molecular structures, although the degradation of micro-pollutants in AOPs has already been investigated, it is still necessary to compare the efficiency of HO• and SO_4•$^-$-based oxidation for specific pollutants under various conditions.

The purpose of this study was to systematically compare HO•-based and SO_4•$^-$-based AOPs for the mineralization of the emerging contaminants in different water matrices. UV/peroxydisulfate (UV/PDS) and UV/H_2O_2 systems were selected because they were among the most common SO_4•$^-$- and HO•-based AOPs, respectively (Shah et al. 2013; He et al. 2014; Xiao et al. 2016). The pesticide atrazine (ATZ), the antibiotic triclosan (TCS), and the odorant 2,4,6-trichloroanisole (TCA) were used as model pollutants. They all have long half-life and are most widely detected in the drinking water environment (Arnold et al. 1995; Chen et al. 2011; de la Casa-Resino et al. 2012; Vlachos et al. 2008; Vestner et al. 2010). Seriously, they pose a long-term threat to ecosystems and human health (Chalew and Halden 2009; Dann and Hontela 2011; Prat et al. 2011). The effect of key factors such as various oxidant concentrations, micro-pollutant initial concentration, different pH conditions, and the most common anions (i.e., Cl^- and CO_3^{2-}/HCO_3^-) on the mineralization efficiency was evaluated. The several reaction rate constants of those three pollutants towards SO_4•$^-$ and HO• were also determined in this study. These results will be helpful to better understand the degradation of micro-pollutants in UV/PDS and UV/H_2O_2 processes, as well as the contribution of secondary radicals in the degradation processes.

Materials and methods

Chemicals and reagents

Chemical standard atrazine (ATZ, purity > 99%), 2,4,6-trichloroanisole (TCA, purity > 98%), triclosan (TCS, purity > 99%), H_2O_2 solution (35%, v/v), and benzoic acid were purchased from Sigma-Aldrich Chemical Co. Ltd. (USA). Peroxydisulfate (PDS), sodium hydroxide, perchloric acid, sodium thiosulfate, sodium carbonate, and sodium chloride were of ACS reagent grade and obtained from Sinopharm Chemical Reagent Co. Ltd. China. Suwannee River natural organic matter (NOM) was obtained from the International Humic Substances Society. Acetonitrile (ACN) and acetic acid of HPLC grade were purchased from Fisher Scientific for ATZ, TCA, and TCS determination. All solutions were prepared with Milli-Q water from a Millipore Water Purification System.

Analytical methods

Concentrations of ATZ, TCA, and TCS were analyzed using a high-performance liquid chromatography (HPLC, Waters 2695) system equipped with a symmetry C18 column (4.6 × 150 mm, 5 μm particle size, Waters) and a photodiode array detector (PDA, Waters 2998). The mobile phase consisted of water (1‰ acetic acid) and acetonitrile (40:60 for ATZ, TCA, and TCS) at a flow rate of 1.0 mL min^{-1} and the sample injection volume was 100 μL. The UV wavelengths for the measurement of ATZ, TCA, and TCS were set at 221 nm, 290 nm, and 230 nm, respectively. Solution pH was measured by a pH meter (PH3-3C, Shanghai precision Instrument CO. Ltd.). H_2O_2 and PDS concentrations were measured by the iodometric method (American Public Health Association

et al. 1915). Multi 3100 N/C TOC analyzers (Analytic jena, German) were used to determine the concentration of natural organic matter (mgC·L^{-1}) according to ISO-8245.

Experimental procedures

The photochemical process was conducted using a bench-scale UV apparatus, consisting of four low-pressure Hg UV lamps (254 nm, GPH212t5l/4, 10 W, Heraeus) housed in a shuttered box, with a vertical tube extending from the bottom. The light travels through the collimated tube down into a 100 mL sample, which is magnetically stirred in a cylindrical glass dish (6 cm diameter × 6 cm deep) 30 cm from the tube. The photon flux (I_0, 253.7 nm) from the ultraviolet light source into the solution was determined by iodide-iodate chemical photometric method to be 1.291×10^{-7} Einstein·L^{-1} s^{-1} and UV irradiance used in this study was 0.16 mW cm^{-2} after calibration. All experiments were carried out in deionized water at a controlled temperature (20 ± 1 °C) and certain time (10 min). Solution pH was buffered at pH 5.0 to 9.0 using 10 mM phosphate and adjusted with NaOH or $HClO_4$. Samples (1 mL) were withdrawn at certain time intervals and quenched by adding 20 μL of sodium thiosulfate. All experiments were conducted in duplicated with the relative standard deviation of less than 5%.

Determination of the second-order rate constants of SO_4^{-}• and HO• with ATZ, TCA, and TCS

In order to determine the second-order rate constants for the reaction between ATZ, TCA, and TCS with SO_4•$^-$ and HO•, benzoic acid (BA) was used as a reference compound according to the competition kinetics, the concentration of the target pollutant (i.e., ATZ, TCS, and TCA) and the competitive reagent (i.e., BA) were in the same order of magnitude (i.e., 5 μM). The constant reaction rates between SO_4•$^-$ and HO• with BA were 1.2×10^9 M^{-1} s^{-1} and 5.9×10^9 M^{-1} s^{-1} (Buxton et al. 1988; Guan et al. 2011), respectively. The reaction rate kinetic constants of ATZ, TCA, and TCS with SO_4•$^-$ and HO• were determined during the UV/PDS and UV/H_2O_2 processes, respectively. 5 mM t-butanol (TBA) was added to the reaction to scavenge HO• produced in UV/PDS process, because the reaction rate constant for TBA and HO• ($k_{HO•,\ TBA}$=6.0×10^8 M^{-1} s^{-1}) (Buxton et al. 1988) is much higher than that with SO_4•$^-$ ($k_{SO_4^{-},TBA}$ =4.0×10^5 M^{-1} s^{-1}) (Neta and Huie 1988). The target substances degradation kinetics can be calculated by the following Eq. (1) (Li et al. 2018; Lu et al. 2018):

$$\ln\frac{[com]_0}{[com]_t} - k_{directi,uv}t = \frac{k_{SO_4^{-}/HO•,\ com}}{k_{SO_4^{-}/HO•,\ BA}} ln\frac{[BA]_0}{[BA]_t} \quad (1)$$

where *com* is the ATZ, TCA, and TCS, respectively, $k_{direct,uv}$ is the observed rate constants for those three compounds degradation by UV irradiation, $k_{SO_4^{-}/HO•,\ com}$ is the second-order rate constants of SO_4•$^-$ and HO• with ATZ, TCA, and TCS, and $k_{SO_4^{-}/HO•,\ BA}$ is the second-order rate constants of SO_4•$^-$ and HO• with BA.

Results and discussion

Reaction rate constants of SO_4^{-}• and HO• with ATZ, TCA, and TCS

The active substances in UV/PDS and UV/H_2O_2 processes including SO_4^{-}• and HO• play a major role in the degradation of target substances. The plot of $\ln\frac{[com]_0}{[com]_t} - k_{directi,uv}t$ and $ln\frac{[BA]_0}{[BA]_t}$ yielded a straight line with a slope of $\frac{k_{SO_4^{-}/HO•,\ com}}{k_{SO_4^{-}/HO•,\ BA}}$ in Fig. 1. The determined second-order rate constants of these three compounds with SO_4•$^-$ and HO• (i.e., $k_{SO_4^{-}}$ and $k_{HO•}$) are shown in Table 1.

According to the above results, the second-order rate constants of ATZ and TCA with SO_4•$^-$ and HO• were not affected by pH in the range of pH 5 to 9, this mainly being because ATZ and TCA could not get ionized when the pH was in the range of 5 to 9 (the pK_a of ATZ and the K_{ow} of TCA is 1.68 and 4.11, respectively). However, the pKa of TCS is 7.9 (Karnjanapiboonwong et al. 2010), TCS mainly exists in the form of deprotonation when the pH is 9, and the second-order rate constants of SO_4•$^-$ and HO• with the deprotonation form of TCS were obtained much higher than that of the molecular form of TCS.

Effect of oxidant dosage

Figure 2 shows the effects of oxidant dosage (100–500 mM) on the ATZ, TCA, and TCS degradation by the UV/H_2O_2 and UV/PDS processes, respectively. For UV/H_2O_2, when the H_2O_2 dosage increased from 100 to 500 μM, after 10 min of reaction, the ATZ, TCA, and TCS removal rates were increased from 40.2 to 63.2%, 65.7 to 77.8%, and 39.9 to 47.5%, respectively. For UV/PDS systems, the ATZ, TCA, and TCS removal rates were increased by 33.8%, 18.8%, and 21.3%, respectively. These results indicated that the ATZ, TCA, and TCS degradation rates increased with increasing oxidant dosage. Similar observations were also reported in previous studies where an increase in PDS and H_2O_2 concentration levels could correspondingly promote the degradation rate of carbamazepine in water (Deng et al. 2013). Notably, the removal rates of ATZ, TCA, and TCS by UV/PDS was about 20~30% higher than that by UV/H_2O_2 under the same oxidant dosage. According to the results above, the reaction

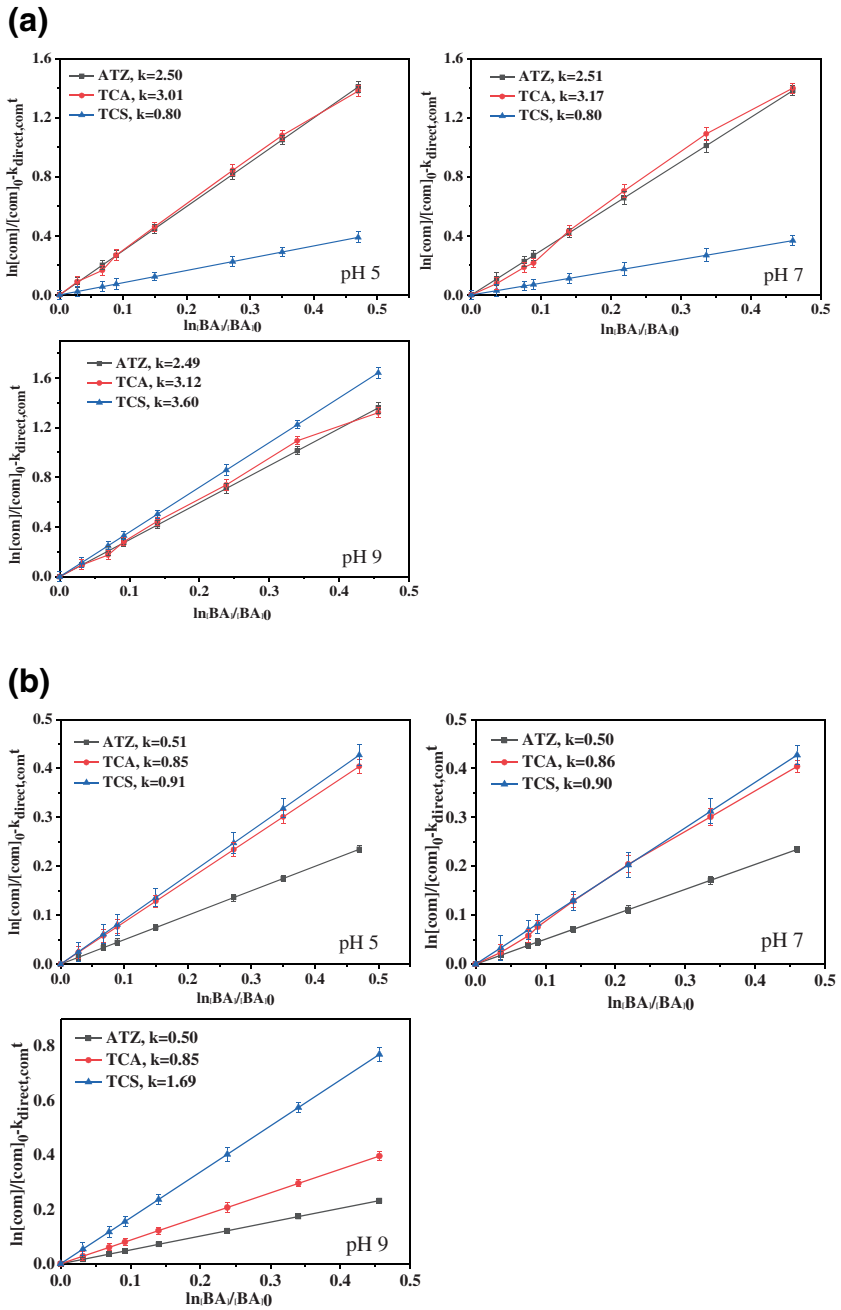

Fig. 1 Determination of the reaction rate constants of $SO_4^{\bullet-}$ (**a**) and HO• (**b**) reacting with ATZ, TCA, and TCS in different solution pH value (pH = 5, pH = 7, pH = 9). Conditions: [ATZ] = [TCS] = [BA] = [TCA] = 5 μM, [PDS] = [H_2O_2] = 500 μM, 10 mM phosphate buffer, $I_0 = 1.291 \times 10^{-7}$Einstein L^{-1} s^{-1}, reaction time = 10 min

Table 1 The second-order rate constants (M^{-1} s^{-1}) of ATZ, TCA, and TCS with $SO_4^{\bullet-}$ and HO•

	pH = 5		pH = 7		pH = 9	
	$k_{SO_4^{\bullet-}}$	$k_{HO\bullet}$	$k_{SO_4^{\bullet-}}$	$k_{HO\bullet}$	$k_{SO_4^{\bullet-}}$	$k_{HO\bullet}$
ATZ	3.0×10^9	3.0×10^9	3.01×10^9	2.95×10^9	2.98×10^9	2.95×10^9
TCA	3.61×10^9	5.0×10^9	3.81×10^9	5.1×10^9	3.74×10^9	5.0×10^9
TCS	0.96×10^9	5.4×10^9	0.96×10^9	5.3×10^9	4.32×10^9	9.97×10^9

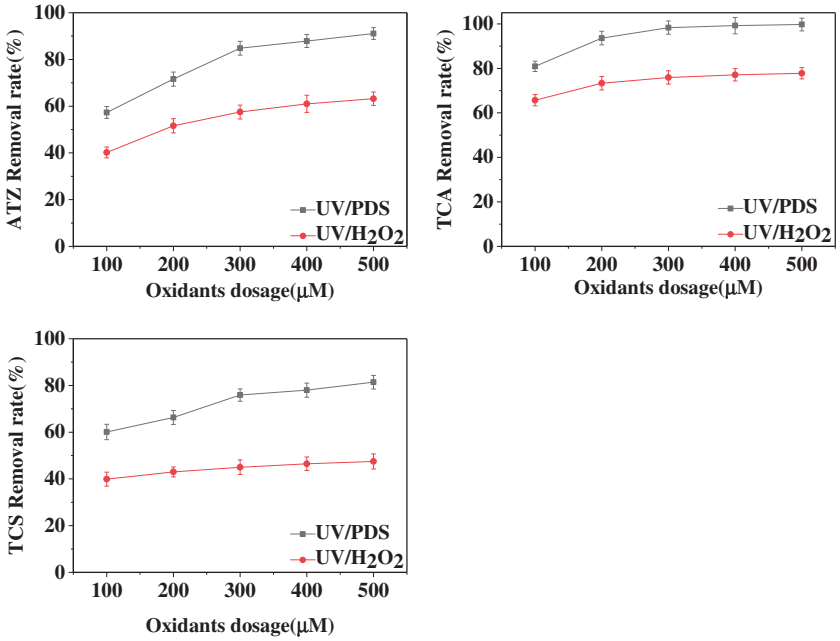

Fig. 2 Effect of oxidants dosage for ATZ, TCA, TCS degradation by UV/PDS and UV/H_2O_2. Conditions: [ATZ] = [TCS] = 2 μM, [TCA] = 200 nM, 10 mM phosphate buffer at pH 7, I_0 = 1.291×10^{-7}Einstein·L^{-1} s^{-1}, reaction time = 10 min

rates of HO• with these three targets are the same order of magnitude as SO_4•$^-$ (Table 1), but the molar adsorption coefficient and quantum yields of PDS (i.e., $\Phi = 0.7$ mol·Einstein^{-1},$\varepsilon = 21.1$ M^{-1} cm^{-1}) is higher than H_2O_2 (i.e., Φ = 0.5 mol·Einstein^{-1}, $\varepsilon = 18$ M^{-1} cm^{-1}) (Yang et al. 2010; Zhang et al. 2015). Therefore, the catalytic efficiency of PDS by UV irradiation was higher than that of H_2O_2 in this study, leading to the higher steady-state concentrations of SO_4•$^-$ in UV/PDS than HO• in UV/H_2O_2 under the same conditions.

Besides, some previous studies have found that the efficiency of UV/H_2O_2 was higher than that of UV/PDS. Tan et al. found that the degradation efficiency of acetaminophen in UV/H_2O_2 was higher than that in UV/PDS (Tan et al. 2014). It was mainly because the second-order rate constant of the reaction between acetaminophen with SO_4•$^-$ was lower than that of the reaction between acetaminophen with HO•.

Effect of the initial ATZ, TCA, and TCS concentration

ATZ, TCA, and TCS degradation were evaluated at different initial concentrations in the UV/H_2O_2 and UV/PDS systems, respectively. As it could be seen in Fig. 3, the degradation rates of ATZ, TCA, and TCS in both systems decreased with the increase of the initial concentration. For example, when the ATZ concentration increased from 0.5 to 5 μM in UV/H_2O_2, the degradation of ATZ decreased from 67.1 to 35.8% after 10 min, while it decreased from 89.9 to 42.8% in the UV/PDS system. At the initial concentration of each target, the UV/PDS degradation efficiency was higher than that of UV/H_2O_2.

These results were consistent with some previous reports, mainly because (i) the increase in micro-pollutant concentration reduced the UV transmission efficiency of the solutions, resulted in the decrease of HO• and SO_4•$^-$ steady-state concentration; and (ii) the increasing intermediate oxidation products improved the scavenge effect on radicals. For instance, recent research indicated that the second-order rate constants of parent ATZ and its primary oxidation products (e.g., Atraimine, DEA, DIA, terbuthylazine, and propazine) with HO• and SO_4•$^-$ were comparable (i.e., 10^9 M^{-1} s^{-1}) (Lutze et al. 2014). The intermediate oxidation products of TCA and TCS (e.g., chlorobenzoquinone, chlorophenol) have also been proved that they have strong ability to scavenge HO• and SO_4•$^-$.

Effect of NOM

In source water, the concentration of NOM is usually at the level of mgC·L^{-1}. Figure 4 shows the effects of NOM on ATZ, TCA, and TCS degradation. As it could be seen, when the dosage of NOM increased from 0.2 to 5.0 mgC·L^{-1}, the degradation of ATZ, TCA, and TCS was significantly inhibited by NOM in both UV/H_2O_2 and UV/PDS processes.

The inhibitory effect of NOM on ATZ, TCA, and TCS degradation could be explained as the following: (i) NOM would exert an inner filter effect for the photolysis of H_2O_2 and PDS, the molar extinction coefficient of NOM was detected to be 0.11 L·mgC^{-1}·cm^{-1} (Luo et al. 2016), (ii) NOM reacted with SO_4•$^-$ and HO• as radical scavenger. In addition, previous studies reported that SO_4•$^-$ or HO• reacted with certain organic compounds (e.g., aromatics, ketones, esters, and aliphatics) by electron transfer to generate organic free

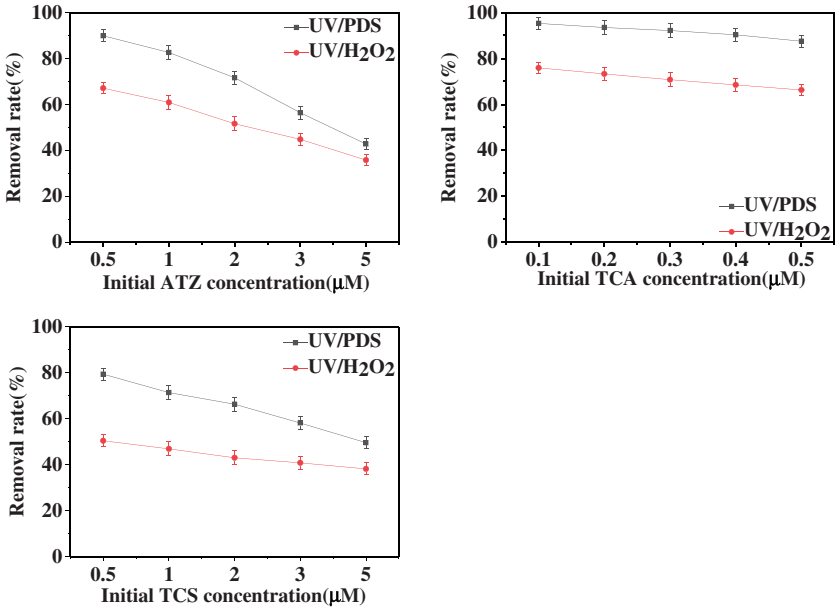

Fig. 3 Effect of initial concentrations of ATZ, TCA, TCS degradation by UV/PDS and UV/H_2O_2. Conditions: [PDS] = [H_2O_2] = 200 μM, 10 mM phosphate buffer at pH 7, $I_0 = 1.291 \times 10^{-7}$ Einstein·L^{-1} s^{-1}, reaction time = 10 min

radicals. However, these organic free radicals have been shown to be much less reactive than $SO_4^{\bullet -}$ or HO•. Besides, Fig. 4 indicates that the removal rates of ATZ, TCA, and TCS in UV/PDS were higher than that in UV/H_2O_2 under the same NOM concentrations. One of the reasons was that the second-order rate constants of NOM reacting with HO• is one order of magnitude higher than that of $SO_4^{\bullet -}$, as shown in Eqs. (2–3) (Lee et al. 2007; Lutze et al. 2015).

$$SO_4^{\bullet -} + \mathrm{NOM} \rightarrow \mathrm{products} \rightarrow k = 6.8 \times 10^3 \left(\mathrm{L\ mgC^{-1}\ s^{-1}}\right) \quad (2)$$

$$\mathrm{HO\bullet} + \mathrm{NOM} \rightarrow \mathrm{products}\ \ k = 2.5 \times 10^4 \left(\mathrm{L\ mgC^{-1} s^{-1}}\right) \quad (3)$$

Effect of pH

The degradation of ATZ, TCA, and TCS by UV/H_2O_2 and UV/PDS at various pH values were carried out, respectively. As shown in Fig. 5, when the solution pH increased from 5 to 9, a significant role in lowering ATZ and TCA removal was exhibited in UV/PDS (i.e., 86.1% vs 46.2% for ATZ, 99.9% vs 67.7% for TCA). However, the increasing pH had a slight inhibitory effect on the degradation of ATZ and TCA in UV/H_2O_2. Different from this, TCS degradation was inhibited both in these two processes when pH ranged from 5 to 8, but it was greatly promoted at pH 9. For example, the removal rates of TCS were 43% and 63.7% at pH 8 in UV/H_2O_2 and UV/PDS, respectively, while which were increased to 59.5% and 86.8% at pH 9.

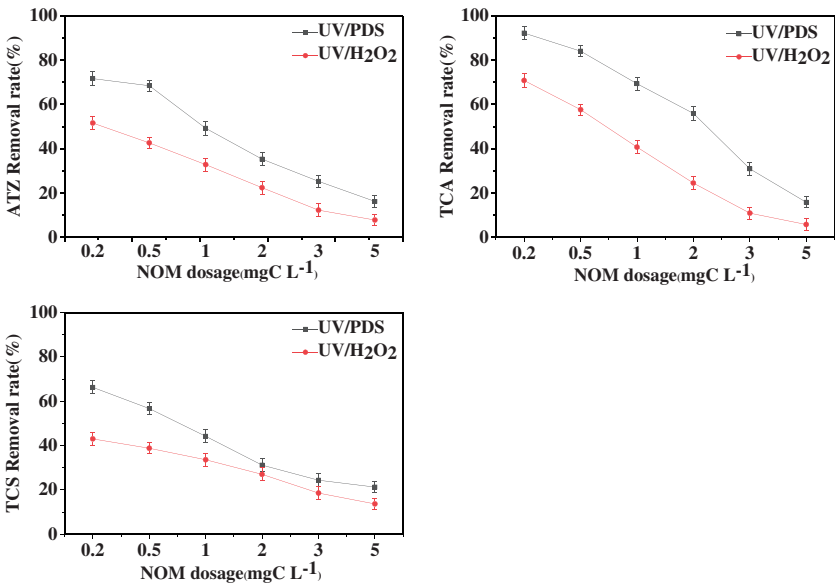

Fig. 4 Effect of NOM for ATZ, TCA, TCS degradation by UV/PDS and UV/H_2O_2. Conditions: [PDS] = [H_2O_2] = 200 μM, [ATZ] = [TCS] = 2 μM, [TCA] = 200 nM, 10 mM phosphate buffer at pH 7, $I_0 = 1.291 \times 10^{-7}$ Einstein·L^{-1} s^{-1}, reaction time = 10 min

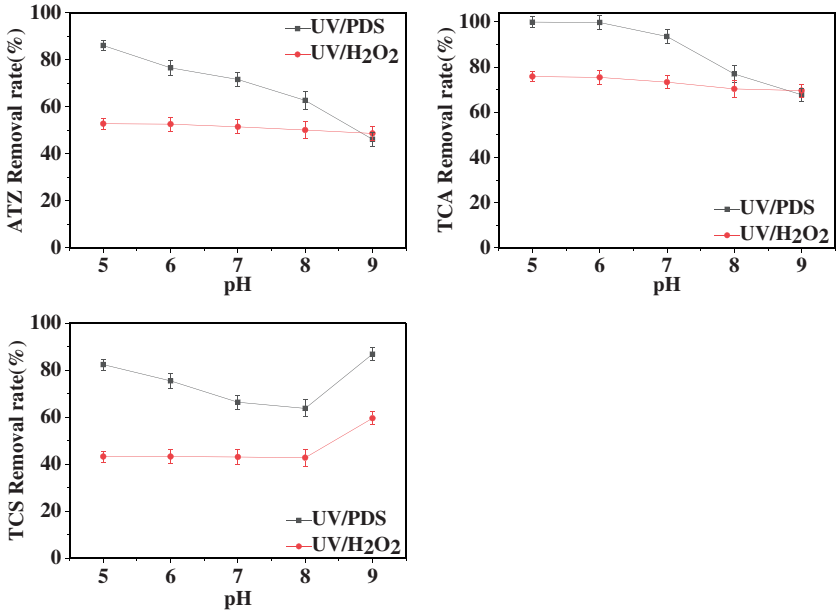

Fig. 5 Effect of pH for ATZ, TCA, TCS degradation by UV/PDS and UV/H_2O_2. Conditions: [PDS] = [H_2O_2] = 200 μM, [ATZ] = [TCS] = 2 μM, [TCA] = 200 nM, 10 mM phosphate buffer at pH 7, $I_0 = 1.291 \times 10^{-7}$ Einstein·L^{-1} s^{-1}, reaction time = 10 min

Generally, the quantum efficiency of photodissociation of PDS and H_2O_2 was identical when the pH was range from 5 to 9, and the formation of SO_4•$^-$ and HO• would not be affected by solution pH. As shown in Fig. 1, the reaction rate constants between radicals (i.e., SO_4•$^-$ and HO•) with ATZ and TCA were stable at pH 5.0, 7.0, and 9.0. Actually, there were 10 mM phosphate buffer in these two processes, whose concentration was over at least 50 times more than the concentration of micro-pollutants. The reaction rate constant of SO_4•$^-$ with HPO_4^{2-} is 1.2×10^6 M^{-1} s^{-1}, which is two orders of magnitude higher than that of SO_4•$^-$ with its protonated form $H_2PO_4^-$ (7.2×10^4 M^{-1} s^{-1}) (Luo et al. 2016). Therefore, the percent of HPO_4^{2-} increased dramatically when pH increased from 5 to 9, leading to increasing the consumption of SO_4•$^-$ in UV/PDS process. The reaction rate constant between HO• and HPO_4^{2-} (1.5×10^5 M^{-1} s^{-1}) is slightly higher than that between HO• and $H_2PO_4^-$ (2.0×10^4 M^{-1} s^{-1}) (Luo et al. 2016). The scavenging capacity of phosphate buffer is less affected by solution pH.

Unlike ATZ and TCA, the pK_a of TCS is 7.9 (Karnjanapiboonwong et al. 2010), the percentage of TCS anionic state in aqueous solution increased suddenly with increasing pH from 8.0 to 9.0. The anionic state of TCS has a higher molar absorption coefficient; the rate constants of anionic state of TCS with HO• and SO_4•$^-$ (9.97×10^9 M^{-1} s^{-1} and 4.32×10^9 M^{-1} s^{-1}, respectively) are higher than those of molecular state of TCS (5.3×10^9 M^{-1} s^{-1} and 0.96×10^9 M^{-1} s^{-1}, respectively.).

Effect of CO_3^{2-}/HCO_3^-

Figure 6 shows the removal rates of ATZ, TCA, and TCS under various CO_3^{2-}/HCO_3^- concentrations in UV/H_2O_2 and UV/PDS, respectively. As it could be seen, the removal rates of ATZ and TCA decreased with increasing CO_3^{2-}/HCO_3^- in both processes. For example, ATZ decreased from 44.8% and 67.6% to 25% and 35% in UV/H_2O_2 and UV/PDS processes, respectively, when CO_3^{2-}/HCO_3^- concentrations increased from 0.5 to 10 mM. In particular, when CO_3^{2-}/HCO_3^- concentrations was less than 2 mM, the removal rates of TCS dropped by 10% and 6% in UV/H_2O_2 and UV/PDS processes, respectively. As the CO_3^{2-}/HCO_3^- dosage increased gradually, the degradation rate of TCS had a slight promotion effect both in the UV/H_2O_2 and UV/PDS processes.

Usually, the presence of CO_3^{2-}/HCO_3^- could reduce the degradation efficiency of micro-pollutants (e.g., ATZ, TCA), which was because CO_3^{2-}/HCO_3^- could scavenge both HO• and SO_4•$^-$ at relative high reaction, and the inhibition effect on HO• was much stronger than that on SO_4•$^-$ (e.g., the second-order rate of bicarbonate with HO• is 8.6×10^6 M^{-1} s^{-1} and that with SO_4•$^-$ is 1.6×10^6 M^{-1} s^{-1}) (Buxton et al. 1988; Zuo et al. 1999; Lai et al. 2017). Therefore, CO_3^{2-}/HCO_3^- showed a stronger inhibitory effect on the degradation of targets in the UV/H_2O_2 process than UV/PDS process.

On the other hand, significant amounts of HO• and SO_4•$^-$ react with CO_3^{2-}/HCO_3^- to form the milder oxidant (CO_3•$^-$, 1.57 ± 0.03 V vs.NHE) (as shown in Eqs. 4–7) (Buxton al. 1988; Zuo et al. 1999). In comparison with HO• and SO_4•$^-$, CO_3•$^-$, as a secondary radical, has a stronger selectivity for target oxidation. The rate constants for the reactions involving CO_3•$^-$ are in the range of 10^2~10^9 M^{-1} s^{-1} (Yan et al. 2019). Previous studies reported that the CO_3•$^-$ was found to primarily react with some electron-rich compounds (e.g., phenols, amines, and sulfur compounds). These results in this study suggested that CO_3•$^-$ was less reactive with ATZ and TCA,

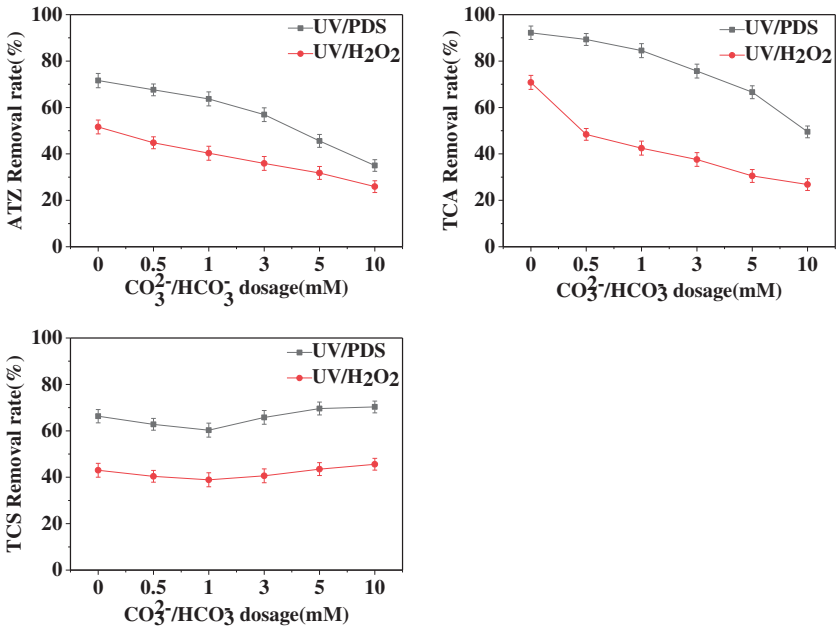

Fig. 6 Effect of CO_3^{2-}/HCO_3^- for ATZ, TCA, TCS degradation by UV/PDS and UV/H_2O_2. Conditions: [PDS] = [H_2O_2] = 200 μM, [ATZ] = [TCS] = 2 μM, [TCA] = 200 nM, 10 mM phosphate buffer at pH 7, I_0 = 1.291×10^{-7} Einstein·L^{-1} s^{-1}, reaction time = 10 min

but the reactivity of $CO_3^{\bullet-}$ with TCS was relativity higher.

$$HO^{\bullet} + HCO_3^- \rightarrow H_2O + CO_3^{\bullet-} \quad k = 8.6 \times 10^6 M^{-1}s^{-1} \quad (4)$$

$$HO^{\bullet} + CO_3^{2-} \rightarrow OH^- + CO_3^{\bullet-} \quad k = 3.9 \times 10^8 M^{-1}s^{-1} \quad (5)$$

$$SO_4^{\bullet-} + HCO_3^- \rightarrow SO_4^{2-} + HCO_3^{\bullet-} \quad k = 1.6 \times 10^6 M^{-1}s^{-1} \quad (6)$$

$$SO_4^{\bullet-} + CO_3^{2-} \rightarrow SO_4^{2-} + CO_3^{\bullet-} \quad k = 6.1 \times 10^6 M^{-1}s^{-1} \quad (7)$$

Effect of Cl^-

The influence of Cl^- on ATZ, TCA, and TCS degradation by UV/H_2O_2 and UV/PDS was investigated at Cl^- concentrations ranging from 0.5 to 10 mM (Fig. 7). For UV/PDS process, Cl^- had a significant inhibitory effect on the degradation of ATZ and TCS. When Cl^- concentrations increased from 0 to 10 mM, after 10 min of reaction, ATZ and TCS degradation decreased by 24.0% and 33.1%, respectively. While, the inhibitory effect of Cl^- on the degradation of TCA was relatively small. Cl^- had little effect on the degradation of ATZ, TCA, and TCS by UV/H_2O_2 process. When Cl^- concentrations increased from 0 to 10 mM, after 10 min of reaction, the removal rates of ATZ, TCA, and TCS had only dropped 4.9%, 4.3%, and 4.6%, respectively.

For UV/PDS process, the second-order rate constants of Cl^- with $SO_4^{\bullet-}$ is 3.1×10^8 M^{-1} s^{-1} at pH = 7 (Neta and

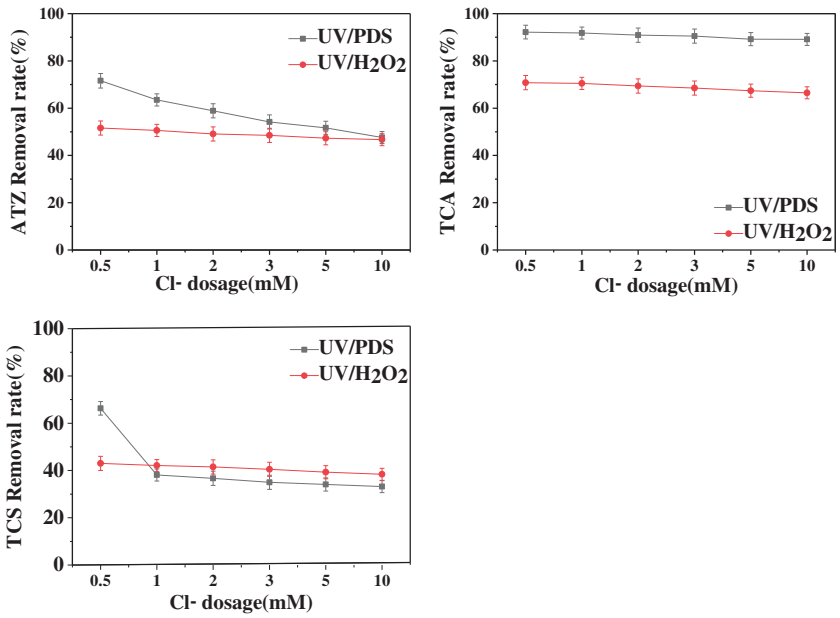

Fig. 7 Effect of Cl^- for ATZ, TCA, TCS degradation by UV/PDS and UV/H_2O_2. Conditions: [PDS] = [H_2O_2] = 200 μM, [ATZ] = [TCS] = 2 μM, [TCA] = 200 nM, 10 mM phosphate buffer at pH 7, I_0 = 1.291×10^{-7} Einstein·L^{-1} s^{-1}, reaction time = 10 min

Huie 1988). Usually, the fast reaction of $SO_4^{\bullet-}$ with Cl^- yields $Cl^\bullet$ and $Cl_2^{\bullet-}$ as shown in Eqs. 8 and 13 (Fang et al. 2014). Similar to $CO_3^{\bullet-}$, these second radical species have strong selectivity for the oxidation of organic matter (Kwon et al. 2018). For example, the secondary rate constant of $Cl_2^{\bullet-}$ with 2-propanol is only $1.5 \times 10^5\ M^{-1}\ s^{-1}$, while the secondary rate constant with hydroquinone is as high as $1.5 \times 10^9\ M^{-1}\ s^{-1}$ (Neta and Huie 1988; Fang et al. 2014).

On the other hand, the presence of Cl^- in the UV/PDS process could promote the conversion of $SO_4^{-}\bullet$ to HO•. Wu et al. used Fe(III)-ethylenediamine-N,N′-disuccinic acid to catalyze PDS to produce $SO_4^{\bullet-}$ to degrade 4-bromophenol (Wu et al. 2015). They found that when 10 mM Cl^- was present, the steady-state concentration of $SO_4^{\bullet-}$ in the system was only 8.0×10^{-14} M, while the steady-state concentration of HO• could reach 3.7×10^{-12} M (Fang et al. 2014). In this study, the reaction rates of $SO_4^{\bullet-}$ and HO• with ATZ, TCA, and TCS were of the same order of magnitude at pH 7, so $SO_4^{\bullet-}$ to HO• conversion had little effect on target degradation.

In this study, the inhibitory effect of Cl^- on ATZ and TCS degradation could be explained as the low reactivity with these two compounds of those secondary reactive chlorine radical species than that of $SO_4^{\bullet-}$ in UV/PDS process. Nevertheless, those secondary reactive chlorine radical species might have similar reactivity with TCA and $SO_4^{\bullet-}$. For UV/H_2O_2 process, the presence of Cl^- scavenging for HO• was apparently weak, which was ascribed to the fast-backward reaction process in the equilibrium reaction of Cl^- with HO• to form $ClOH^{\bullet-}$ (i.e., Eqs. 9) (Neta and Huie 1988; Fang et al. 2014).

$$SO_4^{-}\bullet + Cl^- \rightarrow Cl^\bullet + SO_4^{2-} \quad k = 3.0 \times 10^8 M^{-1}s^{-1} \tag{8}$$

$$HO^\bullet + Cl^- \rightarrow ClOH^{\bullet-} \quad k_+ = 4.3 \times 10^9 \quad k = 6.0 \times 10^9 M^{-1}s^{-1} \tag{9}$$

$$Cl^\bullet + HO^- \rightarrow ClOH^{\bullet-} \quad k = 1.8 \times 10^{10} M^{-1}s^{-1} \tag{10}$$

$$ClOH^{\bullet-} \rightarrow HO^\bullet + Cl^- \quad k = 6.0 \times 10^9 M^{-1}s^{-1} \tag{11}$$

$$ClOH^{\bullet-} + H^+ \rightarrow Cl^\bullet + H_2O \quad k_+ = 2.1 \times 10^{10} \quad k = 2.5 \times 10^5 M^{-1}s^{-1} \tag{12}$$

$$Cl^\bullet + Cl^- \rightarrow Cl_2^{\bullet-} \quad k = 8.5 \times 10^9 M^{-1}s^{-1} \tag{13}$$

$$Cl_2^{\bullet-} + OH^- \rightarrow Cl^- + ClOH^{\bullet-} \quad k = 4.5 \times 10^7 M^{-1}s^{-1} \tag{14}$$

Conclusion

In this work, ATZ, TCA, and TCS removal efficiencies by UV/PDS and UV/H_2O_2 were evaluated under different experimental conditions. Increasing oxidant dosage and decreasing micro-pollutant initial concentration were observed to enhance the degradation of ATZ, TCA, and TCS. The presence of NOM and Cl^- had inhibitory effects on ATZ, TCA, and TCS in both processes. pH affected both the contribution of $SO_4^{\bullet-}$ and HO• and dissociation species in solutions. UV/PDS degrading ATZ and TCA was affected by solution pH and was significant reduced in alkaline solutions, but the change was not obvious in UV/H_2O_2. For TCS, the degradation rate was found to be the lowest at pH 8 and increased dramatically at pH 9 in UV/PDS and UV/H_2O_2. The presence of CO_3^{2-}/HCO_3^- had a small inhibitory effect on ATZ and TCA degradation but promoted the degradation of TCS significantly (> 2 mM) in UV/H_2O_2 and UV/PDS processes. Results of this study also demonstrate that UV/PDS effectively eliminates ATZ, TCA, and TCS with much higher efficacy than UV/H_2O_2.

Funding information This work was financially supported by the National Natural Science Foundation of China (51908335 and 51908334), Natural Science Foundation of Shandong Province (ZR2018BEE036), National Key Research and Development Program of China (2017YFF0209903), and the Doctoral Research Fund of Shandong Jianzhu University (XNBS1822).

References

Ahmed MM, Chiron S (2014) Solar photo-Fenton like using persulphate for carbamazepine removal from domestic wastewater. Water Res 48:229–236

Arnold SM, Hickey WJ, Harris RF (1995) Degradation of atrazine by Fenton's reagent: condition optimization and product quantification. Environ Sci Technol 29(8):2083–2089

American Public Health Association, American Water Works Association, Water Pollution Control Federation, Water Environment Federation (1915) Standard methods for the examination of water and wastewater. American Public Health Association

Bennedsen LR, Muff J, Søgaard EG (2012) Influence of chloride and carbonates on the reactivity of activated persulfate. Chemosphere 86(11):1092–1097

Betarbet R, Sherer TB, MacKenzie G, Garcia-Osuna M, Panov AV, Greenamyre JT (2000) Chronic systemic pesticide exposure reproduces features of Parkinson's disease. Nat Neurosci 3(12):1301–1306

Buxton GV, Greenstock CL, Helman WP, Ross AB (1988) Critical review of rate constants for reactions of hydrated electrons, hydrogen atoms and hydroxyl radicals (·OH/·O^- in aqueous solution. J Phys Chem Ref Data 17(2):513–886

Can ZS, Çakır E (2010) Treatability of organic constituents in the Paşaköy wastewater treatment plant effluent by O_3 and O_3/H_2O_2. Ozone-Sci Eng 32(3):209–214

Chalew TEA, Halden RU (2009) Environmental exposure of aquatic and terrestrial biota to triclosan and triclocarban1. J Am Water Resour As 45(1):4–13

Chen H, Bramanti E, Longo L, Onor M, Ferrari C (2011) Oxidative decomposition of atrazine in water in the presence of hydrogen peroxide using an innovative microwave photochemical reactor. J Hazard Mater 186(2–3):1808–1815

Dann AB, Hontela A (2011) Triclosan: environmental exposure, toxicity and mechanisms of action. J Appl Toxicol 31(4):285–311

de la Casa-Resino I, Valdehita A, Soler F, Navas JM, Perez-Lopez M (2012) Endocrine disruption caused by oral administration of atrazine in European quail (Coturnix coturnix coturnix). Comp Biochem Phys C 156(3–4):159–165

Deng J, Shao Y, Gao N, Deng Y, Zhou S, Hu X (2013) Thermally activated persulfate (TAP) oxidation of antiepileptic drug carbamazepine in water. Chem Eng J 228:765–771

Fang J, Fu Y, Shang C (2014) The roles of reactive species in micropollutant degradation in the UV/free chlorine system. Environ Sci Technol 48(3):1859–1868

Guan Y, Ma J, Li X, Fang J, Chen L (2011) Influence of pH on the formation of sulfate and hydroxyl radicals in the UV/peroxymonosulfate system. Environ Sci Technol 45(21):9308–9314

Haag WR, Yao CCD (1992) Rate constants for reaction of hydroxyl radicals with several drinking water contaminants. Environ Sci Technol 26(5):1005–1013

He X, Pelaez M, Westrick JA, O'Shea KE, Hiskia A, Triantis T, Kaloudis T, Stefen MI, Cruz AA, Dionysiou DD (2012) Efficient removal of microcystin-LR by UV-C/H2O2 in synthetic and natural water samples. Water Res 46(5):1501–1510

He X, Mezyk SP, Michael I, Fatta-Kassinos D, Dionysiou DD (2014) Degradation kinetics and mechanism of β-lactam antibiotics by the activation of H_2O_2 and $Na_2S_2O_8$ under UV-254nm irradiation. J Hazard Mater 279:375–383

Huber MM, Canonica S, Park G, Gunten UV (2003) Oxidation of pharmaceuticals during ozonation and advanced oxidation processes. Environ Sci Technol 37(5):1016–1024

Huerta-Fontela M, Galceran MT, Ventura F (2011) Occurrence and removal of pharmaceuticals and hormones through drinking water treatment. Water Res 45(3):1432–1442

Karnjanapiboonwong A, Morse AN, Maul JD, Anderson TA (2010) Sorption of estrogens, triclosan, and caffeine in a sandy loam and a silt loam soil. J Soils Sediments 10(7):1300–1307

Kattel E, Trapido M, Dulova N (2017) Oxidative degradation of emerging micropollutant acesulfame in aqueous matrices by UVA-induced H_2O_2/Fe^{2+} and $S_2O_8^{2-}/Fe^{2+}$ processes. Chemosphere 171:528–536

Kwon M, Yoon Y, Kim S, Jung Y, Hwang T, Kang J (2018) Removal of sulfamethoxazole, ibuprofen and nitrobenzene by UV and UV/chlorine processes: a comparative evaluation of 275 nm LED-UV and 254 nm LP-UV. Sci Total Environ 637-638:1351–1357

Lai WW, Hsu M, Lin AY (2017) The role of bicarbonate anions in methotrexate degradation via UV/TiO_2: mechanisms, reactivity and increased toxicity. Water Res 112:157–166

Lee C, Yoon J, Gunten UV (2007) Oxidative degradation of N-nitrosodimethylamine by conventional ozonation and the advanced oxidation process ozone/hydrogen peroxide. Water Res 41(3):581–590

Li R, Kong J, Liu H, Chen P, Su Y, Liu G, Lv W (2018) Removal of indomethacin using UV–vis/peroxydisulfate: kinetics, toxicity, and transformation pathways. Chem Eng J 331:809–817

Liu CS, Shih K, Sun CX, Wang F (2012) Oxidative degradation of propachlor by ferrous and copper ion activated persulfate. Sci Total Environ 416:507–512

Liu C, Wu B, Chen XE (2018) Sulfate radical-based oxidation for sludge treatment: a review. Chem Eng J 335:865–875

Lu X, Shao Y, Gao N, Chen J, Deng H, Chu W, An N (2018) Investigation of clofibric acid removal by UV/persulfate and UV/chlorine processes: kinetics and formation of disinfection byproducts during subsequent chlor(am)ination. Chem Eng J 331:364–371

Luo C, Jiang J, Ma J, Pang S, Liu Y, Song Y, Guan C, Li J, Jin Y, Wu D (2016) Oxidation of the odorous compound 2,4,6-trichloroanisole by UV activated persulfate: kinetics, products, and pathways. Water Res 96:12–21

Luo C, Ma J, Jiang J, Liu Y, Song Y, Yang Y, Guan Y, Wu D (2015) Simulation and comparative study on the oxidation kinetics of atrazine by UV/H_2O_2, UV/HSO_5^- and UV/$S_2O_8^{2-}$. Water Res 80:99–108

Lutze HV, Bakkour R, Kerlin N, Von Sonntag C, Schmidt TC (2014) Formation of bromate in sulfate radical based oxidation: mechanistic aspects and suppression by dissolved organic matter. Water Res 53:370–377

Lutze HV, Bircher S, Rapp I, Kerlin N, Bakkour R, Geisler M, Von Sonntag C, Schmidt TC (2015) Degradation of chlorotriazine pesticides by sulfate radicals and the influence of organic matter. Environ Sci Technol 49(3):1673–1680

Main KM, Mortensen GK, Kaleva MM, Boisen KA, Damgaard IN, Chellakooty M, Schmidt IM, Suomi A, Virtanen HE, Petersen JH, Andersson A, Toppari J, Skakkebæk NE (2005) Human breast milk contamination with phthalates and alterations of endogenous reproductive hormones in infants three months of age. Environ Health Persp 114(2):270–276

Neta P, Huie RE (1988) Rate constants for reactions of inorganic radicals in aqueous solution. J Phys Chem Ref Data 17(3):1027–1284

Peter A, Von Gunten U (2007) Oxidation kinetics of selected taste and odor compounds during ozonation of drinking water. Environ Sci Technol 41(2):626–631

Prat C, Besalú E, Baneras L, Anrico E (2011) Multivariate analysis of volatile compounds detected by headspace solid-phase microextraction/gas chromatography: a tool for sensory classification of cork stoppers. Food Chem 126(4):1978–1984

Richardson SD, Ternes TA (2005) Water analysis: emerging contaminants and current issues. Anal Chem 77(12):3807–3838

Rodríguez-Chueca J, Amor C, Fernandes JR, Tavares PB, Lucas MS, Peres JA (2016) Treatment of crystallized-fruit wastewater by UV-A LED photo-Fenton and coagulation–flocculation. Chemosphere 145:351–359

Shah NS, He X, Khan HM, Khan JA, O'Shea KE, Boccelli DL, Dionysiou DD (2013) Efficient removal of endosulfan from aqueous solution by UV-C/peroxides: a comparative study. J Hazard Mater 263:584–592

Shao B, Chen D, Zhang J, Wu Y, Sun c (2009) Determination of 76 pharmaceutical drugs by liquid chromatography - tandem mass spectrometry in slaughterhouse wastewater. J Chromatogr A 1216(47):8312–8318

Sung Y, Li T, Huang S (2005) Analysis of earthy and musty odors in water samples by solid-phase microextraction coupled with gas chromatography/ion trap mass spectrometry. Talanta 65(2):518–524

Tan C, Gao N, Zhou S, Xiao Y, Zhuang Z (2014) Kinetic study of acetaminophen degradation by UV-based advanced oxidation processes. Chem Eng J 253:229–236

Tobergte DR, Curtis S (2013) Scrutinizing pharmaceuticals and personal care products in wastewater treatment. J Chem Inf Model 53:0–9

Vestner J, Fritsch S, Rauhut D (2010) Development of a microwave assisted extraction method for the analysis of 2,4,6-trichloroanisole in cork stoppers by SIDA–SBSE–GC–MS. Anal Chim Acta 660(1–2):76–80

Vlachos P, Stathatos E, Lyberatos G, Lianos P (2008) Gas-phase photocatalytic degradation of 2,4,6-trichloroanisole in the presence of a nanocrystalline Titania film. Applications to the treatment of cork stoppers. Catal Commun 9(10):1987–1990

Wu Y, Bianco A, Brigante M, Dong W, Sainte-Claire PD, Hanna K, Mailhot G (2015) Sulfate radical photogeneration using Fe-EDDS: influence of critical parameters and naturally occurring scavengers. Environ Sci Technol 49(24):14343–14349

Xiao Y, Zhang L, Zhang W, Lim K, Webster RD, Lim T (2016) Comparative evaluation of iodoacids removal by UV/persulfate and UV/H_2O_2 processes. Water Res 102:629–639

Xie P, Ma J, Liu W, Zou J, Yue S, Li X, Wiesner MR, Fang J (2015) Removal of 2-MIB and geosmin using UV/persulfate: contributions of hydroxyl and sulfate radicals. Water Res 69:223–233

Xu X, Li X (2010) Degradation of azo dye Orange G in aqueous solutions by persulfate with ferrous ion. Sep Purif Technol 72(1):105–111

Yan S, Liu Y, Lian L, Li R, Ma J, Zhou H, Song W (2019) Photochemical formation of carbonate radical and its reaction with dissolved organic matters. Water Res

Yang S, Wang P, Yang X, Shan L, Zhang W, Shao X, Niu R (2010) Degradation efficiencies of azo dye acid orange 7 by the interaction of heat, UV and anions with common oxidants: persulfate, peroxymonosulfate and hydrogen peroxide. J Hazard Mater 179(1):552–558

Zhang R, Sun P, Boyer TH, Zhao L, Huang C (2015) Degradation of pharmaceuticals and metabolite in synthetic human urine by UV, UV/H_2O_2, and UV/PDS. Environ Sci Technol 49(5):3056–3066

Zuo Z, Cai Z, Katsumura Y, Chitose N, Muroya Y (1999) Reinvestigation of the acid–base equilibrium of the (bi)carbonate radical and pH dependence of its reactivity with inorganic reactants. Radiat Phys Chem 55(1):15–23